Binary Polymer Brush in a Solvent

K. Geoffrey Soga,* Martin J. Zuckermann, and Hong Guo

Centre for the Physics of Materials and Department of Physics, McGill University, Rutherford Building, 3600, rue University, Montréal, Québec, Canada H3A 2T8

Received July 27, 1995; Revised Manuscript Received December 18, 1995[⊗]

ABSTRACT: We have studied the equilibrium structure of a grafted polymer layer composed of two distinct species of homopolymers, the "binary brush", in various solvent conditions. By using a coarse-grained simulation method that involves direct calculation of the Edwards hamiltonian, we are able to simulate much larger systems than would otherwise be possible with a more standard lattice simulation. If the two species are made sufficiently immiscible, we find lateral binary microphase separation over a wide range of solvent conditions. Due to the presence of solvent, we find a stage where the brush expands in a laterally homogeneous manner as immiscibility increases. In this stage, laterally averaged quantities are well-described by a single solvent−related parameter: a modified excluded volume parameter. This is followed by lateral microphase separation in which the brush volume remains relatively constant. In Θ solvent, this phase separation sets in at a degree of immiscibility consistent with a mean field prediction for melt layers. The onset of phase separation is delayed as solvent quality increases. Furthermore, a reduction in solvent quality results in a stronger crossover between mixed and phase-separated configurations. Under poor solvent conditions, we find interesting structural variations as a result of the combination of phase separation from solvent and phase separation of the two species.

Introduction

When linear polymers are end-grafted to a flat surface in good solvent, the effective polymer−polymer repulsion causes the polymer chains to stretch in the direction perpendicular to the grafting surface. For sufficiently high grafting densities, the system becomes a polymer "brush", with the polymers stretching to a height that scales linearly with N, the degree of polymerization of the polymers. The brush height is then considerably greater than the radius of gyration of an isolated grafted polymer, which scales as $N^{3/5}$. End-grafted polymer brushes have been the subject of many investigations, motivated by both the commercial importance and intrinsic physical interest of these layers.[1] The quality of the solvent has an enormous influence on the configurational state of the polymers in the brush. In good solvent, the brush is homogeneous parallel to the grafting surface and can be characterized by a z-dependent monomer density, $c(z)$, where z is the coordinate perpendicular to the grafting plane. In this case, self-consistent field (SCF) theory predicts a parabolic form for $c(z)$.[2,3] Theories using higher order approximations as well as numerical simulations have shown that, while the parabolic form is essentially correct for the interior of the brush, a depletion layer, as predicted by De Gennes,[4] occurs close to the grafting surface and loose polymer ends extend beyond the SCF-determined brush height. In contrast, for the case of a brush immersed in a poor solvent, the lateral symmetry of the brush is broken. Early computer simulations of polymer brushes in poor solvent suggested the possibility of lateral instabilities in the monomer density.[5,6] Subsequent analytical work confirmed this instability,[7,8] and recently an extensive simulation conclusively demonstrated and characterized the large scale structure formed in the unstable regime.[9]

In the present study, we consider two-component polymer brushes, or binary brushes, subject to a demixing interaction parametrized by w_{ab}. Marko and Witten[10] predicted instabilities in a symmetric binary brush composed of immiscible chains under melt conditions and used SCF theory to examine the equilibrium properties. They studied two possible ordered phases for sufficiently high immiscibility: a "rippled" phase described in terms of a "density wave" in composition directed along the surface, which is equivalent to lateral microphase separation, and a "layered" phase rich in one component at the bottom of the brush and rich in the second component at the top of the brush. If the homopolymers were not end-grafted, bulk phase separation[4] would occur for $Ncw_{ab} > 4$, where c is the total monomer density of the brush. Marko and Witten show that lateral microphase separations occurs for $Ncw_{ab} = 9.098$, while the layered phase would be observed in the brush for $Ncw_{ab} = 16$. Thus, the lateral transition preempts the layering transition and is expected to be the one observed. Marko and Witten corroborated the occurrence of microphase transitions in binary brushes by studying real space correlations.[11]

Brown et al.[12] performed large scale Monte Carlo calculations with the polymers represented by self-avoiding walks on a simple cubic lattice in a symmetric binary brush for near-melt conditions, i.e., grafting densities of 0.3 and 0.5 on a surface of area 64×64 with $N = 100$. They observed microphase separation after quenching the system from $w_{ab} = 0$ to $w_{ab} = 2$. This was an impressive computational undertaking, requiring "about one *Sparcstation-year*",[12] to perform two quenches. Another simulation by Brown for the same model by using simulated annealing confirmed this result.[13] Analytical work for binary brushes under melt conditions has since been extended to the strong demixing limit,[14] whereby a self-consistent model of the strongly phase-separated brush containing phase-separated regions and mixed regions was characterized. Lai[15] performed bond-fluctuation Monte Carlo simulations of a binary brush in a good solvent at a lower grafting density of approximately 0.1 on surfaces of area 32×32 and 64×64. N was primarily 20 and 40, with some runs having N's of up to 80. In this case, the equilibrium structures were investigated as a function of w_{ab} and varying relative fraction of the binary types. For the symmetric case of equal fractions, the laterally

[⊗] Abstract published in *Advance ACS Abstracts,* February 15, 1996.

0024-9297/96/2229-1998$12.00/0 © 1996 American Chemical Society

separated phase was again observed. For asymmetric mixtures, layering was observed, with the minority phase segregating to the top of the brush, away from the grafting surface.

In this paper, we study the two-component brush under various solvent conditions. By using a coarse-grained simulation technique where the Edwards free energy function is directly calculated, we are able to investigate large systems, yielding configurations showing unmistakable lateral microphase separation. This method will be described in some detail in the next section. With these advantages, we are able to go beyond the previous work, providing more quantitative details than before. We are further able to consider the effect of varying solvent quality on microphase separation. We see, in marked contrast to the incompressible melt layer, that the presence of solvent allows for a stage of laterally homogeneous volume expansion in the brush as immiscibility increases, well before the onset of microphase separation. Moreover, solvent quality is seen to modulate the lateral microphase separation process itself, even though the binary species are indistinguishable with respect to solvent interactions. Our results for the onset of microphase separation in a Θ solvent agree with a mean field prediction for a melt; however, in good solvent, the onset of microphase separation is delayed. Furthermore, we see evidence that decreasing solvent quality produces a much sharper crossover between mixed configurations and laterally microphase-separated configurations. Finally, we will describe a preliminary qualitative examination of the binary brush in poor solvent conditions.

Methods

The configurational partition function for a system of K polymers with N monomers per polymer is given by

$$Z = \int \delta\{\mathbf{R}_k(n)\}\, e^{-\beta H\{\mathbf{R}_k(n)\}} \tag{1}$$

where $\mathbf{R}_k(n)$ is the position of the nth monomer on the kth polymer. In this work, $H\{\mathbf{R}_k(N)\}$ is taken to be the Edwards hamiltonian, given by[16]

$$H\{\mathbf{R}_k(n)\} = \sum_{k}^{K}\sum_{n}^{N}\left(\frac{3kT}{2b^2}\left(\mathbf{R}_k(n) - \mathbf{R}_k(n-1)\right)^2 + U(\mathbf{R}_k(n))\right) \tag{2}$$

The first term in eq 2 represents the probability distribution of a Gaussian chain, i.e., the bond length probability is Gaussian with zero mean and variance b^2. $U(\mathbf{r})$ is a position dependent potential, and for a binary brush containing two types of monomers, A and B, it is given by

$$U(\mathbf{r}) = \frac{w_2}{2}c^2(\mathbf{r}) + \frac{w_3}{3}c^3(\mathbf{r}) + \frac{w_{ab}}{2}c_a(\mathbf{r})c_b(\mathbf{r}) \tag{3}$$

Here $c_{a,b}(\mathbf{r})$ is the concentration of monomers at the point $\mathbf{r}$, defined self-consistently by

$$c_{a,b}(\mathbf{r}) = \sum_k \int \mathrm{d}n\ \delta(\mathbf{r} - \mathbf{R}_k^{a,b}(n)) \tag{4}$$

where the superscripts and subscripts a and b refer to monomers of type A or B, respectively. Furthermore, $c(\mathbf{r})$ is the total monomer density, equal to $c_a(\mathbf{r}) + c_b(\mathbf{r})$. For future reference, we define the monomer density difference at the point $\mathbf{r}$ as $c_-(\mathbf{r}) = c_a(\mathbf{r}) - c_b(\mathbf{r})$.

The coefficient w_{ab} is the immiscibility coefficient. For negative w_{ab}, there is an effective attraction between monomers of different types, while for positive w_{ab}, the two types of monomers become immiscible. Consequently, within the model described earlier, $w_{ab} = 0$ describes a monodisperse, homogeneous polymer brush, since polymers of types A and B cannot be distinguished. The excluded volume parameter, w_2, determines the interaction of monomers with the solvent, which we take to be the same for monomers of both types. For positive values of w_2, good solvent conditions prevail, while negative w_2 describes poor solvent conditions. The Θ condition is described by $w_2 = 0$. Finally, the parameter w_3 can be regarded as the third virial coefficient and is taken to be positive or zero. It is not relevant in good solvent conditions and will be set to zero for w_2 positive. For poor solvent conditions, it is necessary to bound the free energy from below, and w_3 therefore will be assigned a finite, positive value when w_2 is negative.

To determine the equilibrium properties of this model, we note that the hamiltonian in eq 2 describes a system of point "beads" connected by ideal springs of spring constant $3kT/b^2$ in a potential $U(\mathbf{r})$ described by eq 3. Monte Carlo simulation of the mechanical bead−spring system therefore allows direct measurement of the equilibrium properties of the original polymer system. The Monte Carlo algirithm is implemented as follows. A monomer is selected at random and moved for a random trial distance in a random direction. The energy difference between the previous configuration and the new configuration generated by the trial move is calculated by evaluating eq 2. The trial move is accepted or rejected according to the Metropolis criterion.[17] The concentration that appears in eq 3 is determined by coarse-graining the simulation volume into cubes and counting the number of monomers with each cube. The number of monomers per volume of the cube gives the approximate concentration at all points within the cube.

This manner of simulation has certain advantages over the standard lattice methods typically used in polymer simulations. For example, bond-crossing constraints are not specifically enforced, and excluded volume interactions are accounted for energetically through eq 3. Accounting for these factors geometrically, as is usually required in lattice schemes, is much less efficient. Furthermore, trial moves can be adjusted to optimize the acceptance ratio. Finally, since the hamiltonian of eq 2 is used as the starting point in field theory formulations, direct comparison can be made with analytic results obtained from such theories as no fitting parameters are required. We have used this method to examine the properties of homogeneous end-grafted polymer brushes for both good and poor solvent conditions. The simulation results gave a correct description of the polymer brush in the good solvent case,[18] which compared well with the results found by using SCF theory. Furthermore, the method was particularly successful in investigating lateral microphase separation in a homogeneous polymer brush under poor solvent conditions.[9] The major disadvantage of this method is that the dynamics is unrealistic, restricting its use to equilibrium studies. Also, the starting point of this simulation scheme is a model hamiltonian, and the results thus inherit the assumptions and ap-

proximations of the model. However, for the problem at hand this simulation method is quite adequate.

In this study, we consider linear homopolymers with N monomers per polymer. K polymers are randomly and irreversibly grafted by one end to an impenetrable plane with surface density $\sigma = K/L^2$, where L^2 is the area of the plane in the simulation volume. Half of the K polymers are chosen (randomly) to consist entirely of monomers of type A, with the remainder consisting of monomers of type B. The grafting plane is the xy plane situated at $z = 0$, and periodic boundary conditions are imposed in the directions tangential to this plane. Monomers are confined to the positive half-space $z > 0$, and the top of the simulation box is placed at a large enough value of z to be effectively at infinity. In our simulations, polymers are grafted at a surface density of $\sigma = 0.1$ on a square plane of area either 128×128 or 64×64. Each polymer contains $N = 64$ monomers, and the box size for coarse-graining has linear dimensions of 2. The unit of length is chosen such that $b^2 = 3$.

Results and Discussion

Two sample configurations of the binary brush, obtained from our simulations, are shown in Figure 1. They correspond to different values of the immiscibility parameter w_{ab}, and two views are presented for each configuration. The upper diagram in each case is the edge-on perspective, viewed parallel to the grafting plane, while the lower diagram is the view from above, looking perpendicularly down toward the grafting plane. Black lines represent polymers of type A, while gray lines represent polymers of type B.

Figure 1a is a typical configuration in the absence of immiscibility, i.e., $w_{ab} = 0$. In this case, both the total monomer density and the distribution of monomers of types A and B should be homogeneous. Indeed, in both views, monomers of types A and B appear evenly distributed. Figure 1b is a typical configuration for large w_{ab}. Strong immiscibility is expected in this case, and the view from above clearly shows lateral phase segregation, resulting in microphase-separated domains rich in either A or B type monomers. Note that the side view gives no indication of layering, as monomers of different types do not visibly segregate in the vertical direction. As will be discussed in more detail later, the average domain width is approximately one-quarter of the lattice size, which corresponds to twice the lateral end-to-end distance of a polymer in a Θ solvent.

These results lead to the same phenomenology reported in previous work,[12,15] from which the following consistent picture emerges. For small values of w_{ab}, entropic effects dominate, favoring the laterally homogeneous state. However, for sufficiently large immiscibility, energetic effects dominate the entropic effects, causing the polymers to phase-separate into A-rich and B-rich domains. If the grafting points were free to move, the phase separation would continue until macrophase separation into single domains of A and B separated by one interface occurred. However, due to the irreversible end-grafting of each polymer onto the grafting surface, macrophase separation cannot take place and the equilibrium structure consists of local domains of single polymer species. Since the polymers fluctuate laterally over a distance of approximately twice the polymer end-to-end distance, it is plausible that the domains should have the same size. If the lateral density is sufficiently high (as is expected in a brush), excluded volume interactions will be screened and the end-to-end distance will be that expected for a Θ solvent. This argument for the selection of domain size where lateral patterns are formed in polymer brushes is quite general and has been observed in such cases as lateral microphase separation in poor solvent[7–9] and binary brush melts,[10,12] as well as binary brushes

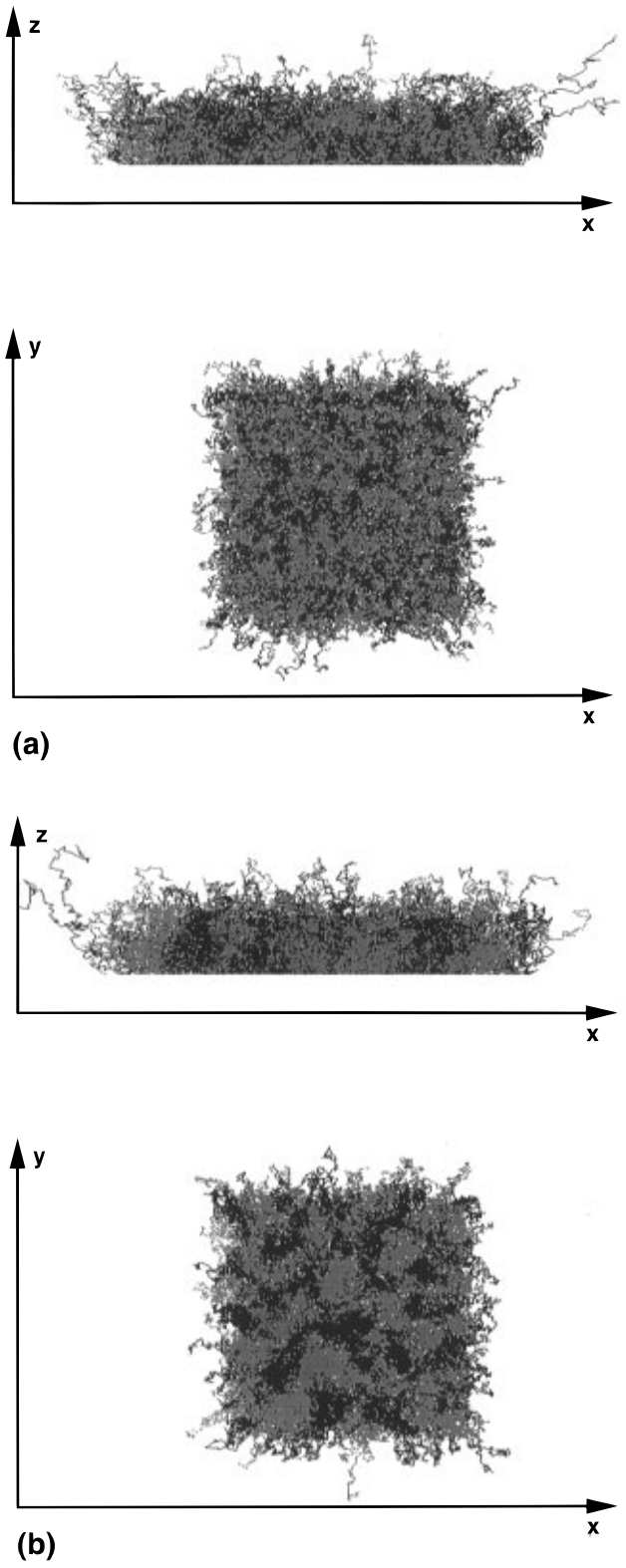

Figure 1. Sample configurations of the two-component polymer brush for (a) $w_2 = 0.5$, $w_{ab} = 0.0$ (no immiscibility), and (b) $w_2 = 0.5$, $w_{ab} = 1.5$. The upper figure is an edge view, parallel to the grafting plane, while the bottom figure is the view down along the z axis toward the top of the brush. The system size is $L = 128$ and the grafting density is $\sigma = 0.1$.

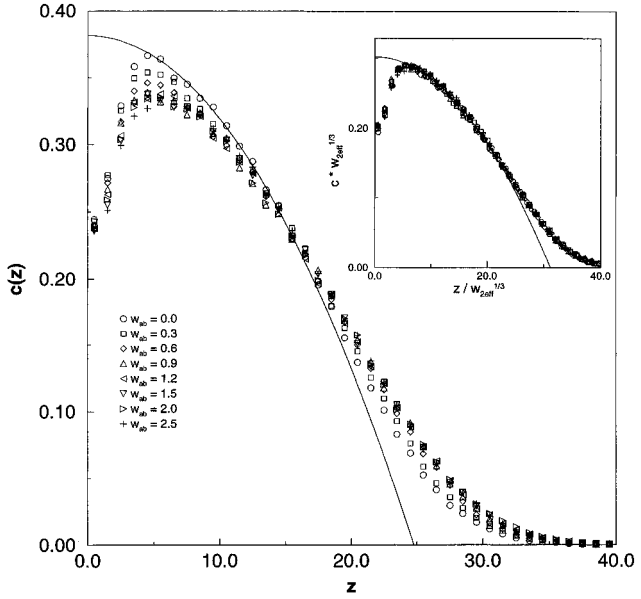

Figure 2. Total monomer density profiles for different values of w_{ab}, with solvent quality fixed at $w_2 = 0.5$. The line corresponds to an analytical prediction from SCF theory. The case of $w_{ab} = 0$ is indicated by open circles. The inset shows the profiles for different w_{ab} values scaled with an effective good solvent parameter, w_{2eff}. The system size is $L = 128$ and the grafting density is $\sigma = 0.1$.

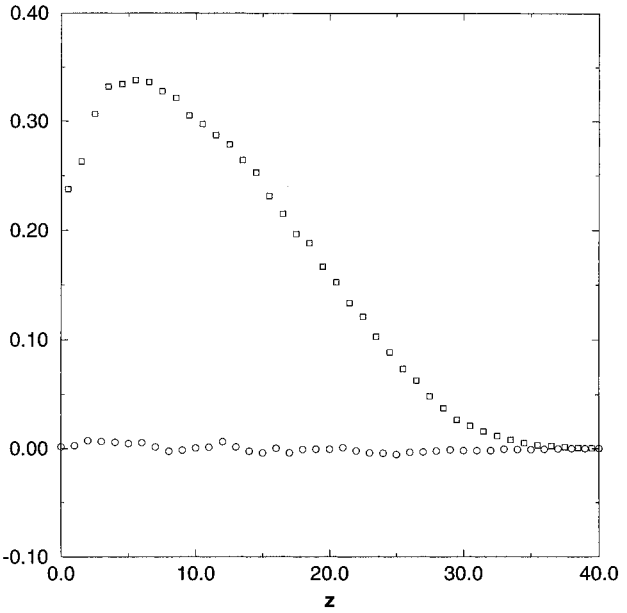

Figure 3. Profile of the monomer density difference for $w_{ab} = 1.5$, $w_2 = 0.5$, corresponding to the configuration in Figure 1b. The total density profile is also shown to provide a scale. For all z, the density difference is negligible compared to the density in the layer. The small variation shows little vertical segregation. The system size is $L = 128$ and the grafting density is $\sigma = 0.1$.

at lower density as shown in ref 15 and in this work.

To make contact with previous theoretical results for end-grafted polymer brushes, we next examine monomer density distributions as a function of z, the perpendicular distance away from the grafting surface. We define the monomer density profile, $c(z)$, to be

$$c(z) = \frac{1}{L_x L_y}\int_0^{L_y}\int_0^{L_x} c(x,y,z)\,dx\,dy \qquad (5)$$

where c is the total monomer density. The definition is identical for the monomer density difference, $c_-(z)$. L_x and L_y are the dimensions of the grafting surface in the x and y directions, respectively.

Density profiles for the total monomer density are shown in Figure 2 for various degrees of immiscibility. Small but systematic changes are evident as w_{ab} is increased. The particular case of $w_{ab} = 0$ corresponds to a binary brush with no differential interactions between A and B type polymers and is therefore equivalent to a homogeneous brush. In this case, there is an analytical prediction from SCF theory[2] for the density profile:

$$c(z) = \frac{\pi^2}{8w_2N^2}\left[N^2\left(\frac{12\sigma w_2}{\pi^2}\right)^{2/3} - z^2\right] \qquad (6)$$

The solid line in Figure 2 gives the SCF result of eq 6. The resulting agreement with the simulation data is the same as that found by Laradji et al.[18] for $w_{ab} = 0$. That is, there is good agreement except for the depletion zone near the wall and the smooth tail at the top edge of the brush. We note that there are no free parameters to adjust when comparing the data with the expected profile. This highlights one of the advantages of the current simulation method stated in the Introduction: parameters of the simulation can be formulated directly in terms of polymer field theory.

As w_{ab} is increased from zero, there is a small but distinct tendency for the profile to flatten out, suggesting that the polymers stretch away from the surface as the repulsion between A and B polymer types increases. Because a more favorable polymer interaction with the solvent would have qualitatively the same effect, we reinterpret the enhanced immiscibility as an increase in solvent quality. An increase in the value of w_{ab} thus modifies w_2, creating an effective value, $w_{2eff} > w_2$. Note that eq 6 becomes independent of w_2 given the change of variables $c \rightarrow w_2^{1/3}c$ and $z \rightarrow z/w_2^{1/3}$. We assume this to be a good solvent scaling form. Thus, if the data can be described in terms of varying solvent quality, we expect that a rescaling of the profile data using $c \rightarrow w_{2eff}^{1/3}c$ and $z \rightarrow z/w_{2eff}^{1/3}$ should result in data collapse onto a universal curve for appropriate values of w_{2eff}. The results are shown in the inset in Figure 2, and we do indeed find convincing data collapse for all values of w_{ab}.

This rescaling does not follow directly from previous work since eq 6 was derived by assuming a laterally featureless brush; in fact, the analysis of Marko and Witten[10] was restricted to the weak segregation limit so that the classical trajectories $z(n)$, where n gives the position of a monomer on a polymer chain, would not be affected by segregation effects. However, there are clear indications from Figure 1b and the following discussion that phase separation has occurred over the range in which we fit w_{2eff}, giving rise to clear lateral microphase structure. Nonetheless, the brush appears to remain laterally homogeneous on *average*, even after the onset of microphase separation, as seen in the profile for the density difference, c_-, shown in Figure 3 for the phase-separated configuration of Figure 1b. The total density profile, c, is also shown in this figure to provide a scale. The figure shows that there is negligible variation in the c_- profile, its value being close to zero, indicating no significant monomer excess of either type for any value of z. This may help to explain why laterally averaged quantities, such as the density profile, are well-described by a single parameter, in this case the modified excluded volume parameter, w_{2eff}. In

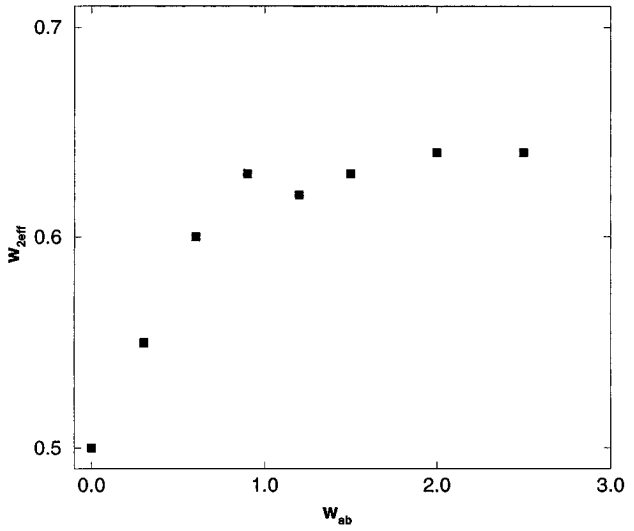

Figure 4. Effective excluded parameter w_{2eff} determined from the scaling of the total monomer density profile (Figure 2) as a function of w_{ab}. w_{2eff} appears to begin saturating at $w_{ab} \simeq 1.0$. The system size is $L = 128$ and the grafting density is $\sigma = 0.1$.

addition, the lack of variation in the c_- profile shows that there is no vertical phase segregation, supporting previous findings that microphase separation is completely lateral.

The fitted values of w_{2eff} are shown in Figure 4 as a function of w_{ab}. The increase in effective solvent quality with increasing immiscibility can be clearly seen for small values of w_{ab}. For larger values, however, w_{2eff} becomes independent of w_{ab}. To explain why w_{2eff} saturates, we propose that the process of microphase separation advances in two stages. As immiscibility is increased, we suppose that there is a range of w_{ab} values before the onset of microphase separation where the energy added to the brush is compensated for by an overall lowering of the brush density achieved by stretching the polymers away from the surface. For w_{ab}'s greater than a particular value, microphase separation sets in and any further increase in immiscibility energy will, to a certain extent, be compensated for by the lateral rearrangement of the monomers. Since this is a lateral ordering process, it does not necessarily require brush expansion, and therefore no further increase should be seen in w_{2eff}. As a more direct probe of the brush expansion, we measured the value of z averaged over all monomers in the system as an indication of brush height. Results are given in Figure 5. As a function of w_{ab}, we see that there is indeed a stage where the height increases, implying a volume expansion. This is followed by a stage where the rate of expansion is markedly decreased, suggesting saturation. For $w_2 = 0.5$, the saturation begins at the same value of w_{ab} where w_{2eff} began to saturate (Figure 4).

For a more detailed study of the lateral structure, we calculate the Fourier transform of the plane-projected monomer density difference:

$$\hat{c}_-(q_x,q_y) = \int dx\, dy \left(\int c_-(x,y,z)\, dz\right) e^{i(q_x x + q_y y)} \quad (7)$$

to obtain the two-dimensional structure factor

$$S(q_x,q_y) = \hat{c}_-(q_x,q_y)\hat{c}_-^*(q_x,q_y) \quad (8)$$

In Figure 6, we show structure factor results circularly averaged for different values of w_{ab} for a constant value

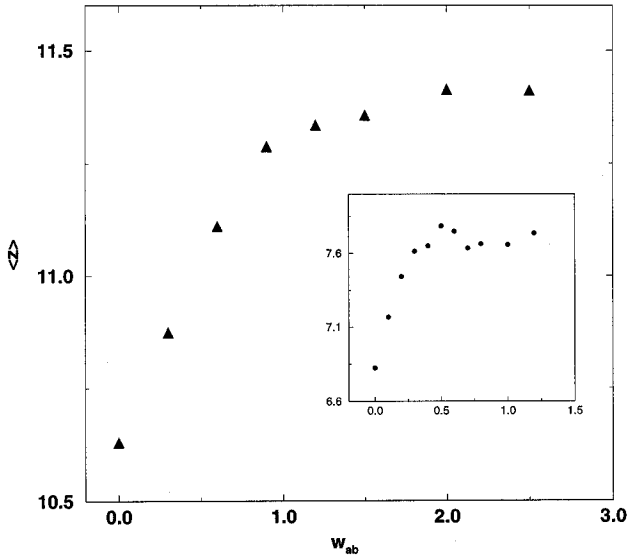

Figure 5. Average monomer z value, as a measure of the brush height, plotted as a function of w_{ab} (▲) for $w_2 = 0.5$ and $L = 128$. The dependence of the average z on w_{ab} is qualitatively similar to that of w_{2eff} in Figure 4. The same plot is shown for $w_2 = 0.0$, $L = 64$ in the inset (●).

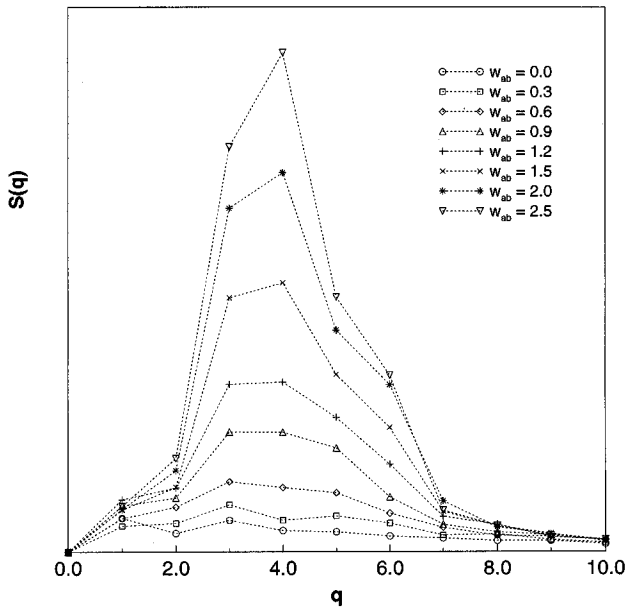

Figure 6. Structure factors of the laterally projected monomer density difference for different values of w_{ab}. The results shown here are circularly averaged. The value of q is given in units of $1/L$, where L is the system size. A peak appears in the structure factor at $q = 4$ corresponding to the average domain separation in the microphase-separated state. The system size is $L = 128$ and the grafting density is $\sigma = 0.1$. The solvent quality is fixed at $w_2 = 0.5$.

of w_2 corresponding to good solvent. Each structure factor is the result of averaging over five equilibrium configurations.[19] The appearance of a peak in the structure factor at a nonzero value of q suggests that a new length scale emerges as w_{ab} increases (when the two species become sufficiently immiscible), and it becomes more prominent as w_{ab} is increased. This clearly corresponds to the structure that develops as microphase separation sets in. The value of q associated with the peak in the structure factor thus corresponds to the length scale determined by this local structure. In particular, we expect the peak to correspond the average separation between domains. This is indeed the case as the periodic spacing between the micro-

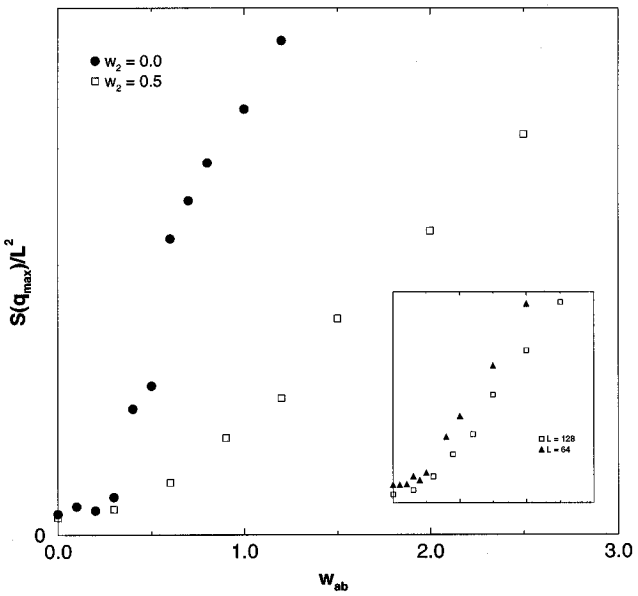

Figure 7. Values of $S(q)$ for q corresponding to the order formed in the microphase-separated state as an indicator of microphase separation: ●, $L = 64$, $w_2 = 0$; □, structure factors shown in Figure 6. Note that the onset of order is much sharper in the case of $w_2 = 0$. The values of $S(q)$ are normalized by L^2. The inset shows a comparison for two system sizes, $L = 64$ and $L = 128$, for fixed solvent quality $w_2 = 0.5$. Note that there is relatively little system size dependence.

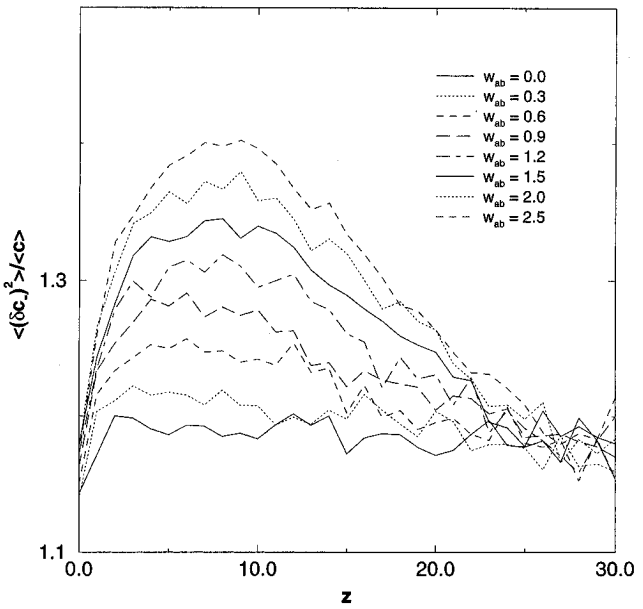

Figure 8. Fluctuations in the density difference per monomer, indicating microphase separation, shown as a function of z for different values of w_{ab}. Microphase separation is strongest where the density profile peaks and is suppressed at the wall, probably due to grafting. The system size is $L = 128$ and the grafting density is $\sigma = 0.1$. The solvent quality is fixed at $w_2 = 0.5$.

domains seen in Figure 1b is consistent with the peak position of the structure factor observed in Figure 6. The average domain spacing is approximately twice the end-to-end distance, projected in the xy plane, of a polymer in Θ solvent. As mentioned earlier, this domain size is consistent with results from previous simulations.[12,15] Note, moreover, that the peak position stays at $q = 4$ for all higher values of w_{ab}. This implies that, unlike phase separation in a binary alloy, almost no coarsening occurs. In fact, the domains seem to appear at a fixed wavelength, which remains constant regardless of the degree of immiscibility. Similar results were obtained in a previous study,[12] where the peak in the structure factor remained constant as one configuration was quenched. Even so, we cannot resolve small changes in the peak position due to the limit of resolution imposed by the finite system size. We remark that structure factors for the total monomer density gave no indication of structure in the total monomer density.

As an indicator of the progress of microphase separation, we use the value of the structure factor at the q value corresponding to the local order formed in the phase-separated regime (i.e., the peak value of $S(q)$). This is plotted in Figure 7 for two cases: a large system with $w_2 = 0.5$ and a smaller system with $w_2 = 0$. For $w_2 = 0.5$, the peak height grows smoothly, suggesting a gradual crossover to microphase-separated states. For $w_2 = 0$ the crossover is much sharper, even though the system size is smaller. In a previous work,[15] the absolute value of the density difference was studied over a wide range of w_{ab} values for $N = 20$ and 40. The authors found no sharpening of the crossover for the case of larger N and, thus, suggested that there was no true phase transition in the thermodynamic limit. However, we believe that a more detailed and more appropriate finite-size scaling analysis is still needed, in which one systematically increases the area of the grafting plane while keeping the grafting density, σ, fixed. In this regard, we can, however, make some comments on the basis of the data shown in the inset of Figure 7. Here the solvent quality is fixed at $w_2 = 0.5$, and results are shown for two system sizes, $L = 128$ and $L = 64$. When these results are normalized by L^2, there is little system size dependence, giving no evidence of a phase transition. In this work we have not performed the finite-size analysis in any detail, since this requires a prohibitively large computational effort. We thus cannot properly address the question of the existence of a thermodynamic phase transition at this time.

As stated in the Introduction, Marko and Witten[10] showed that lateral microphase separation under melt conditions occurs when system parameters are such that $Ncw_{ab} = 9.098$, whereas bulk phase separation[4] occurs when this value is 4 and the ratio of these two values is 2.27. Here c is the average monomer concentration in the brush. Although our simulations were performed for a brush in solvent, a comparison with this prediction is still useful, particularly for the case $w_2 = 0$. From our data, we can estimate c by using $c \simeq N\sigma/2\langle z\rangle$, where $\langle z\rangle$ is the z value averaged over all monomers and $2\langle z\rangle$ is approximately the brush height. For the case of $w_2 = 0$, Figure 5 indicates that microphase separation occurs when $w_{ab} \simeq 0.4$ and $\langle z\rangle \simeq 7.7$, yielding 2.7 for the ratio of Ncw_{ab} between microphase separation in a Θ solvent and bulk phase separation. This value is reasonably close to the predicted value for the melt. On the other hand, when a good solvent is present such as for $w_2 = 0.5$, Figure 5 shows $w_{ab} \simeq 1.0$ and $\langle z\rangle \simeq 11.3$, giving 4.5 for the ratio. This is further evidence that the nature of the solvent has a marked influence on the occurrence of microphase separation.

In Figure 8, we show the mean squared density difference fluctuations per monomer as a function of z. Near the grafting plane, the fluctuations in c_- are strongly suppressed due to the fixing of one end of the polymer on that plane. Otherwise, the tendency for microphase separation appears proportional to the density. Therefore, microphase separation first occurs

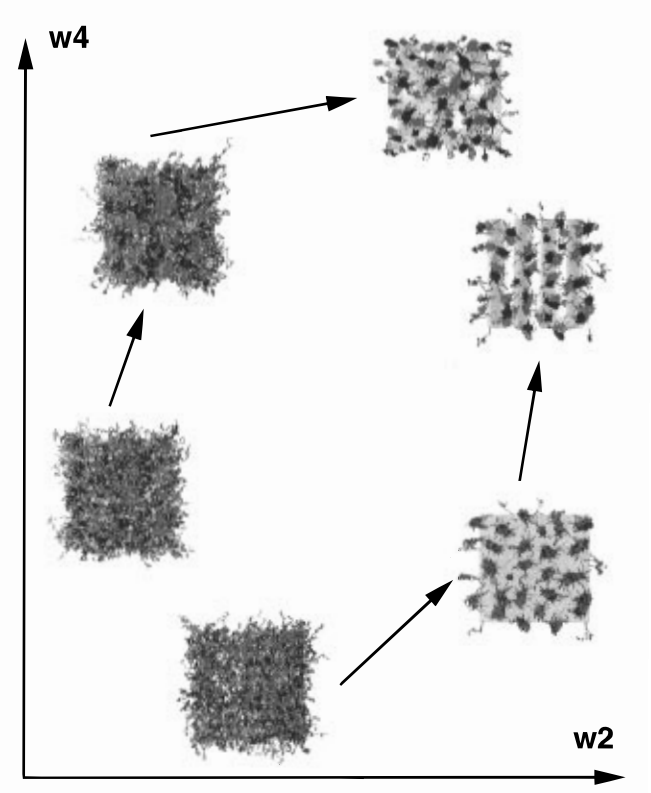

Figure 9. Samples of configurations for the polymer in poor solvent. Two different patterns of annealing are shown. They are, using the notation (w_2, w_3, w_{ab}), (sequence top right) (0, 0.4, 0.2) → (0, 0.4, 1.6) → (−1.2, 0.4, 1.6) and (sequence bottom left) (0, 0.4, 0) → (−1.5, 0.4, 0) → (−1.5, 0.4, 1.2). Intermediate configurations are not shown. The system size is $L = 64$ and the grafting density is $\sigma = 0.1$

in the middle of the brush where the density is highest, and the brush always remains most strongly separated in this region. This is clear evidence that microphase separation does *not* occur uniformly throughout the brush and remains nonuniform for all values of w_{ab}. For the melt case, a "composition oscillation" as a function of z was indeed predicted,[10] although we see clear qualitative differences due to the presence of solvent. The peak of the density difference profile for the "composition oscillation" was predicted to be very close to the top of the brush in the melt case. We find that, in the presence of solvent, the peak corresponds to the maximum of the total monomer density profile and decreases monotonically toward the top of the brush.

Finally, we explore microphase separation in poor solvent conditions for $w_2 < 0$. As is known from previous work,[6−9,15] a homogeneous end-graft polymer brush will undergo a lateral microphase separation of monomers from the surrounding solvent at a sufficiently negative value of w_2, resulting in the formation of microdomains of monomer-rich regions and monomer-poor regions. In the case of an end-grafted binary component brush, two types of microphase separation are possible: microphase separation of monomers from the solvent regardless of type and binary microphase separation due to the immiscibility of the two polymer types. The competition between these two types of microphase separation is expected to produce interesting phase behavior, and we have investigated some of the possibilities in a qualitative fashion. In our simulations, both types of microphase separation were observed but with very different equilibrium structures, depending on the order in which the microphase separations were produced. In Figure 9 we show two cases. If the solvent is first made increasingly poor with no immiscibility, microphase separation of monomers regardless of type from the solvent is induced. Thus, clusters of solvent-separated monomers appear with the expected average cluster spacing, with types A and B mixed evenly in all clusters. As immiscibility is introduced in this solvent-separated state, types A and B phase-separate completely within each cluster. Furthermore, immiscibility can be introduced in good solvent, as before, and increased until the two types microphase-separate at fixed w_2. Now, as the solvent quality is made poor, the monomers indeed separate from the solvent, but in this case, the previously formed binary phase-separated domains determine the nature of the clusters formed as monomers phase-separate from the solvent. The result is the appearance of solvent-separated clusters of pure A type or pure B type.

Summary

In conclusion, we have observed microphase separation of a binary brush due to immiscibility interactions under various solvent conditions. We find that the brush response to increasing immiscibility proceeds in two stages: an overall expansion stage and a microphase separation stage. In the expansion stage, where the immiscibility coefficient w_{ab} is relatively small, the brush relaxes by expanding outward in a laterally uniform fashion. The role of w_{ab} is largely to "renormalize" the excluded volume parameter w_2, and polymers of different type mix very well laterally. We found that the overall density profile in the direction perpendicular to the grafting plane (the z direction) is essentially the same as that of a pure polymer brush if the "renormalized" w_2 parameter is used. At larger values of w_{ab}, it is energetically more advantageous for the two polymer species to undergo microphase separation, and clear microphase separation in the lateral direction is indeed observed. For a Θ solvent, our numerical data for the onset of microphase separation are found to be consistent with predictions based on a mean field model of polymer melts. On the other hand, for good solvent, we found the the onset to be considerably delayed from the melt case. Furthermore, the onset is much more abrupt for poorer solvents. We have also found clear evidence of z dependence in the microphase separation, in that the demixing of the two types of monomers is nonuniform along the z direction. This may explain why the onset is sharper in some cases than in others. Finally, we have also investigated, in a qualitative manner, the phase behavior of the binary brush in a poor solvent. We found different conformations depending on the detailed path for microphase separation. In particular, pure domains of the two different polymer types or mixed domains were observed, depending on whether w_2 or w_{ab} was changed first.

There are still several points that require further consideration. First, as mentioned earlier, a finite-size scaling analysis is required to determine whether or not a true thermodynamic phase transition occurs when the brush becomes laterally inhomogeneous. Since we found that solvent quality plays a vital role, such an analysis should cover a wide range of values of w_2. Second, it would be very useful to carry out an SCF analysis on the model studied here and compare it with the results of our simulations. This would permit the construction of the relevant phase diagram and the prediction of the lateral instability line, as was done for

a homogeneous brush in a poor solvent.[7] Finally, we have found interesting phenomena for the binary brush in the presence of poor solvent, but a full quantitative study should be carried out. We will report these investigations in a future publication.

Acknowledgment. The authors thank Professor Amit Chakrabarti for suggesting this problem and for a stimulating discussion. K.G.S. thanks Dr. Brett Ellman for many helpful discussions. We gratefully acknowledge support by the Natural Sciences and Engineering Research Council of Canada and le Fonds pour la Formation de Chercheurs et l'Aide à la Recherche de la Province de Québec.

References and Notes

(1) Milner, S. T. *Science* **1991**, *251*, 905.
(2) Milner, S. T.; Witten, T. A.; Cates, M. E. *Macromolecules* **1988**, *21*, 2610.
(3) Zhulina, E. B.; Borisov, O. V.; Priamitsyn, V. A. *J. Colloid Interface Sci.* **1990**, *137*, 495.
(4) de Gennes, P.-G. *Scaling concepts in polymer physics*; Cornell University Press: Ithaca, NY, 1979.
(5) Lai, P.-Y.; Binder, K. *J. Chem. Phys.* **1992**, *97*, 586.
(6) Grest, G. S.; Murat, M. *Macromolecules* **1993**, *26*, 3108.
(7) Yeung, C.; Balazs, A. C.; Jasnow, D. *Macromolecules* **1993**, *26*, 1914.
(8) Tang, H.; Szleifer, I. *Europhys. Lett.* **1994**, *28*, 19.
(9) Soga, K. G.; Guo, H.; Zuckermann, M. J. *Europhys. Lett.* **1995**, *29*, 531.
(10) Marko, J. F.; Witten, T. A. *Phys. Rev. Lett.* **1991**, *66*, 1541.
(11) Marko, J. F.; Witten, T. A. *Macromolecules* **1992**, *25*, 296.
(12) Brown, G.; Chakrabarti, A.; Marko, J. F. *Europhys. Lett.* **1994**, *25*, 239.
(13) Brown, G. Ph.D. Dissertation, Kansas State University, 1995.
(14) Dong, H. *J. Phys. II Fr.* **1993**, *3*, 999.
(15) Lai, P.-Y. *J. Chem. Phys.* **1994**, *100*, 3351.
(16) Doi, M.; Edwards, S. F. *The Theory of Polymer Dynamics*; Oxford University Press: New York, 1986.
(17) Binder, K. *Monte Carlo Methods in Statistical Physics*; Springer-Verlag: Berlin, 1979.
(18) Laradji, M.; Guo, H.; Zuckermann, M. J. *Phys. Rev. E* **1994**, *49*, 3199.
(19) We make a cautionary note about equilibrium. When domains begin to form, it is possible that dynamics slow considerably, since rearrangement of the domain structure is a large wavelength process that may have time scales beyond our ability to measure.

MA951102Q